frontiers in Climate

TYPE Original Research
PUBLISHED 21 April 2026
DOI 10.3389/fclim.2026.1761461

Evaluating model uncertainty in critical threshold estimations from time series data: application to the Atlantic meridional Overturning Circulation

Alessandro Cotronei*, Eirik Myrvoll-Nilsen and Martin Rypdal

Department of Mathematics and Statistics, UiT - The Arctic University of Norway, Tromsø, Norway

Check for updates

OPEN ACCESS

EDITED BY
Agus Santoso,
University of New South Wales, Australia

REVIEWED BY
Vanessa Skiba,
Alfred Wegener Institute Helmholtz Centre for Polar and Marine Research (AWI), Germany
Soong-Ki Kim,
Yale University, United States

*CORRESPONDENCE
Alessandro Cotronei
a.cotronei@uit.no

RECEIVED 05 December 2025
REVISED 17 March 2026
ACCEPTED 26 March 2026
PUBLISHED 21 April 2026
CORRECTED 22 April 2026

CITATION
Cotronei A, Myrvoll-Nilsen E and Rypdal M (2026) Evaluating model uncertainty in critical threshold estimations from time series data: application to the Atlantic meridional Overturning Circulation. *Front. Clim.* 8:1761461. doi: 10.3389/fclim.2026.1761461

Analysis of tipping points (rapid, large-scale, and potentially irreversible transitions in Earth system components) is crucial for assessing the resilience of the Earth's subsystems and anticipating risks associated with climate change. Predicting tipping points from time-series data requires accounting for variability, system-specific factors, and high-quality data, which are often limited. Existing approaches, while useful, depend on strong assumptions that may reduce predictive accuracy. In this study, we focus on the model used to approximate system behavior, and argue that modeling assumptions can significantly alter estimates of critical thresholds, and including assessments of whether a system will reach a critical transition at all. We show that, in the case of the Atlantic Meridional Overturning Circulation (AMOC), assuming different polynomial degrees in simple model approximations can lead to entirely different estimates of the critical threshold, or even that no threshold exists. This effect is particularly exacerbated by the interannual variability of the AMOC fingerprints used. These considerations highlight the need for more advanced techniques and increased robustness in model selection and underlying assumptions when interpreting estimates of critical transitions.

KEYWORDS
Atlantic Meridional Overturning Circulation (AMOC), early-warning signals, parameter estimation, saddle-node bifurcation, tipping points

1 Introduction

Tipping points are rapid, large-scale, and possibly irreversible transitions that can occur within the Earth's subcomponents (Armstrong McKay et al., 2022), characterized by the influence of a unique parameter, typically the global temperature (Armstrong McKay et al., 2022; Abrams et al., 2023). Tipping can occur when a system crosses a critical threshold, causing a stable state to disappear, or through noise- or rate-induced mechanisms, where fluctuations or rapid changes trigger transitions that are generally harder to predict (Ritchie and Sieber, 2017). Potential tipping behavior has been identified in several components of the Earth system (Lenton et al., 2008; Kriegler et al., 2009; Lenton, 2013; Wang et al., 2023; Milkoreit et al., 2024).

There exist established Early-Warning Signals (EWS) methods that aim to anticipate impending transitions by detecting features typical of stochastic dynamical systems under the weakening of stability, such as increased variance and autocorrelation, or other characteristics of tipping systems (Scheffer et al., 2009; Dakos et al., 2012; Lenton et al., 2012; Lenton, 2013). These methods rely on simplified model frameworks such as first-order approximations (Scheffer et al., 2009). Early warning signal methodologies are often grounded in critical slowing down, which is observed near tipping points as equilibrium stability weakens. As a dynamical system approaches a critical threshold, its dominant recovery rate decreases, reducing the system's ability to track the stable branch and causing progressively slower recovery from small perturbations (Chisholm and Filotas, 2009; Lenton et al., 2012; Dakos and Bascompte, 2014; Nazarimehr et al., 2020). Statistical EWS, including those presented in this manuscript, exploit this behavior; however, their effectiveness depends on assumptions regarding external forcing and noise structure, and they are therefore prone to false positives and negatives (Boettiger and Hastings, 2012; Kéfi et al., 2013; Dakos et al., 2015; Burthe et al., 2016; Rietkerk et al., 2025). Determining when, or for which values of forcing parameters, a system reaches a tipping point would be an important application of EWS methods. However, such estimates require approaches that account for variability and system-specific factors, as well as the inherent uncertainty in the data, which is constrained by the limitations of the measurements (Ditlevsen and Johnsen, 2010; Ben-Yami et al., 2023). Existing approaches, such as Ditlevsen and Ditlevsen (2023), provide useful starting points, but their reliance on strong assumptions may limit accuracy.

In this study, we focus on the Atlantic Meridional Overturning Circulation (AMOC), which is a suspected tipping element in the Earth system (Armstrong McKay et al., 2022). The AMOC is part of a vast system of ocean currents that functions like a conveyor belt for heat (Barry, 2014). It is primarily driven by variations in temperature and salinity, which influence the density of seawater (Stommel, 1961; Cessi, 1994; Barry, 2014). Warm, salty water flows northward along the surface of the Atlantic, where it gradually cools, becomes denser, and sinks to deeper layers. This deep water then travels southward before rising again in lower latitudes, completing the circulation cycle (Barry, 2014; Rahmstorf, 2024). By redistributing heat across the globe, the AMOC plays a critical role in regulating climate patterns, particularly in Europe (Meccia et al., 2023). A potential shutdown would therefore have large impacts across the globe (Jackson et al., 2015). The AMOC plays a key role in distributing heat and salt throughout the Atlantic Ocean, exporting freshwater and importing salt in the process. This exchange helps maintain the density gradients that drive the circulation. However, when excess freshwater enters the North Atlantic–such as from melting ice or increased precipitation–it can disrupt this balance, reducing surface water density and weakening the overturning. Changing climatic conditions such as increased precipitation due to anthropogenic climate change may further enhance freshwater input, leading to a progressively fresher Atlantic, causing additional weakening of the AMOC, and a potential transition toward a *weak state* (Boers, 2021; Jackson et al., 2023). Such a change could occur much more rapidly than variations observed in the recent history of the system, and may be potentially irreversible. This behavior therefore qualifies as a tipping point (Boers, 2021). The possibility of such tipping is further supported by results from conceptual models (Stommel, 1961; Cessi and Young, 1992; Cessi, 1994), which predict bistable regimes and potential transitions between states driven by temperature and salinity variations. This study integrates the results in Ben-Yami et al. (2023), which show that even a simple quadratic model produces highly uncertain AMOC tipping-time predictions due to gaps and variability in the observational data. We extend this by examining structural model uncertainty, comparing linear, quadratic, and cubic formulations to test whether SPG SST data can distinguish scenarios with or without a bifurcation. Our results show no model is clearly preferred, reinforcing that tipping-time predictions remain fundamentally unconstrained by both data quality and model assumptions.

This paper is structured as follows. In Section 2, we introduce the motivation for our study, the AMOC fingerprint and data, and summarize the methodologies used. In Section 3, we demonstrate how these methods can lead to biased or unreliable predictions of future AMOC behavior, thus highlighting the model uncertainty in tipping predictions. Section 4 discusses the broader implications of these findings. In particular, we advance the following arguments:

- Assumptions underlying low-dimensional approximating models strongly influence conclusions about tipping behavior inferred from observational data.
- Reliable model inference is not possible with the available data. The interannual variability is too large to allow a clear separation between the drift of the stable state and the fluctuations, an assumption underlying most early-warning signal methods. Moreover, physically informed model selection may impose structural constraints that are not supported by the data.

2 Materials and methods

Following Ditlevsen and Ditlevsen (2023), we employ two different methods to estimate the critical threshold. We use statistical indicators, specifically the lag-1 autocorrelation AC(1) to infer the AMOC tipping threshold from SPG SST data. It is based on the fact that if a system approaches a tipping point, autocorrelation AC is expected to reach the unitary value. We also use maximum likelihood estimation to fit given models to the SPG SST data. We show that the results of both methods change when a different model is used. In particular, starting from the normal form of the saddle-node bifurcation. We also show that using a different model degree (e.g., 1–3) can give rise to different estimated scenarios for the AMOC, under all methodologies used in this paper.

2.1 Analysis framework and model setup

Traditional EWS methodology is based on ideas inspired by simple models with few variables (Armstrong McKay et al., 2022).

In most frameworks used in the literature, models are on the form:

$$\dot{x} = f(x) + \lambda + \sigma\eta(t) \tag{1}$$

where x is a scalar state variable, λ the forcing variable, and $\sigma\eta(t)$ represents Gaussian noise. The function $f(x)$ represents how the system dynamically responds to changes in the forcing. In Equation 1, the set of points for which the deterministic component $f(x)+\lambda$ equals zero defines the equilibrium states (fixed point), and by varying λ one can define equilibrium branches. Stable equilibria are those to which the system returns after small perturbations, while unstable points repel trajectories. A stable branch contains information about how the system responds to changes in the control parameter λ. A *bifurcation* occurs when the branch changes in the number or nature of its equilibrium points, marking a qualitative shift in system behavior.

The function $f(x)$ in Equation 1, which we refer to as the model, is often approximated by a polynomial for the purpose of data analysis. Our manuscript mainly focuses on the polynomial model and its degree (i.e., maximal exponent) as a source of uncertainty. We show that different assumptions about the simple models used in the data analysis can lead to different conclusions regarding the future behavior of the AMOC, given the same data. Model uncertainty in the data analysis has a substantial influence on the predicted critical thresholds. In addition, common model simplifications further increase this uncertainty.

2.2 AMOC tipping and data

The possibility of AMOC tipping highlighted by early-warning signals has been already been discussed in the literature (Boers, 2021; Ditlevsen and Ditlevsen, 2023), emphasizing that an abrupt shift might occur within decades or centuries. The results presented in Ditlevsen and Ditlevsen (2023) predict with high confidence an abrupt transition for the AMOC in the time span between the years 2037 and 2109. This result is obtained by analyzing the Subpolar Gyre Sea Surface Temperature (SPG SST), which is considered a representative proxy or fingerprint for the AMOC. Fingerprints of AMOC strength are commonly used because direct measurements are limited in temporal and spatial coverage. These fingerprints are derived from patterns of cooling in the subpolar Atlantic combined with warming in the Gulf Stream region (Caesar et al., 2018), which are considered representative of the underlying AMOC dynamics, including slower water transport. In particular, we use the same dataset as Ditlevsen and Ditlevsen (2023), which spans from 1870 to 2021.

We also use a model realization from van Westen et al. (2024). This dataset corresponds to CESM model output representing the AMOC water transport at 26°N (in Sverdrups). Linearly increasing freshwater is added to the North Atlantic over a period of 2,200 years. In this experiment, tipping behavior is observed after 1,758 years of simulation but shows no easily detectable statistical indicators of tipping close to the critical threshold (van Westen et al., 2024). Additionally, the model exhibits high variability during the initial years (van Westen et al., 2024), which may be comparable to the AMOC fingerprint reported in Ditlevsen and Ditlevsen (2023).

2.3 Filtering techniques

In our analysis, we use standard filtering techniques such as *low-pass* and *high-pass* filters. Low-pass filters are used to isolate long-term trends and slow dynamics in the system, while high-pass filters highlight short-term variability and noise. These tools, commonly employed in time-series analysis, rely on the Fourier transform. The signal is converted to the frequency domain, where frequencies below or above the cut-off are removed, and then transformed back to the time domain (Bloomfield, 1976). The choice of cut-off frequency is critical, as it determines which components of the signal are considered noise vs. meaningful variation. This approach is particularly useful for analyzing climate time series, as it allows the separation of high-frequency noise from the underlying system state, an implicit assumption on which many EWS methods are based.

2.4 Saddle-node bifurcation normal form

The normal form of a saddle-node bifurcation is given by Equation 2:

$$\dot{x} = \lambda - x^2. \tag{2}$$

It describes the universal behavior of a saddle-node bifurcation (characterizing irreversible tipping) and is commonly used in the literature. However, this normal form is derived from Taylor expansion (Scheffer et al., 2009; Strogatz, 2018; Ditlevsen and Ditlevsen, 2023) at the critical point and therefore using it assumes that a tipping point is present. Moreover, it assumes that higher order terms in the expansion can be neglected, and therefore it may be that it approximates well the desired function only in the neighborhood of the expansion point, and it is not necessarily a good approximation for a function at a state far away from its critical transition.

2.5 Cessi model

As a test case with known model degree, we used a simplified and dimensionless Cessi model (Cessi, 1994). Since this model can conceptually describe the behavior of the AMOC collapse we can consider it as physically motivated, in particular with regard to the polynomial degree in the equation, i.e., 3, obtained by multiplying the factors of the equation.

The Cessi model we use is the reduced model described in Cessi (1994), obtained by neglecting temperature effects on the AMOC and considering only the salinity-driven component (Equation 3):

$$dx = \left[\mu(t) - x\left(1 + \eta^2(1-x)^2\right)\right]\frac{1}{\tau_a}\,dt + \sigma\,dW_t, \tag{3}$$

where x is the dimensionless salinity difference, depending on the freshwater influx $\mu(t)$ into the polar box of the model and dW_t

is white noise. The parameters used are chosen to be realistic for the AMOC, following Lux et al. (2022); in particular, $\eta^2 = 4.1234$ represents the most probable value for the ratio between wind-driven spreading of water and the AMOC's self-driven transport. The parameter η^2 governs the bifurcation structure of the model. The freshwater forcing $\mu(t)$ drives the AMOC from pre-industrial values $\mu_0 = 0.8$ (corresponding to an influx of 0.47Sv freshwater toward the Northern box of the model) to tipping $\mu_{\text{final}} = 1.0155$ (5.97Sv) over the integration interval, which is taken in dimensionless units from 0 to 5, with one unit corresponding to 280 years.

Statistical fluctuations are included as in Lux et al. (2022), with noise amplitude $\sigma = 0.3$. We also include the parameter τ, which can be used to artificially increase the response speed of the AMOC to perturbations. In the realistic AMOC model, $\tau = 1$ is implicitly assumed, which leads to a slow response that does not display early-warning signals (EWSs). To illustrate the emergence of EWSs, we accelerate the AMOC response by a factor of 100, choosing $\tau = 1/100$. All the experiments we perform are initialized at equilibrium and integrated with Euler-Maruyama method and time step size 10^{-3}.

2.6 Critical threshold prediction from statistical indicators: AC(1) extrapolation

Statistical methods can help determine the critical threshold of a tipping phenomenon, or the value of the critical forcing at which the tipping or bifurcation occurs. One such method is the AC(1) extrapolation method (Ditlevsen and Ditlevsen, 2023; Ben-Yami et al., 2024). The method is based on estimating the following indicator

$$A|\lambda| = \left(\frac{\ln(\mathrm{AC}(\Delta X))}{2\Delta t}\right)^2, \tag{4}$$

where λ is the forcing parameter, A is a scaling factor, AC((ΔX) is the autocorrelation of the variation ΔX from the equilibrium point and Δt is the time step. A challenge with using statistical indicators for EWS is that effective detrending is required to separate the effects of noise from changes in the mean state, as failing to do so can lead to unreliable estimates and potentially inflating the indicator because of effects of changing state being mixed with the noise. However, achieving this separation may be impossible with the available data. A common approach is linear detrending, see for example Ditlevsen and Ditlevsen (2023). If we assume a normal-form model for the bifurcation the fluctuation dissipation theorem (Ben-Yami et al., 2024) yields (Ditlevsen and Ditlevsen, 2023):

$$A|\lambda| = \left(\frac{\sigma^2}{4\mathrm{Var}(\Delta X)}\right)^2. \tag{5}$$

Also, the variance satisfies the following identity, having an asymptote in correspondence to the critical threshold:

$$\mathrm{Var}(\Delta X_t) \approx \frac{1}{\sqrt{\lambda_c - \lambda}}. \tag{6}$$

The critical threshold λ_c can then be estimated as the intersection of the line that interpolates $1/\mathrm{Var}(\Delta X_t)^2$ with the value zero. For this reason, the Equations 4, 5 decrease linearly toward zero when the critical threshold is reached. However, in the more general case, if the exponent is not necessarily 2, from the theory in Scheffer et al. (2009), the linearized approximation at the equilibrium state satisfies (Equation 7):

$$\gamma^2 = \mathrm{Var}(\Delta x) = \frac{\sigma^2}{2a}, \tag{7}$$

with σ being the standard deviation and $a = -f'(x^*)$ the sensitivity depending on the equilibrium point x^* (Scheffer et al., 2009). If E is an integer, we can consider the equation $\dot{x} = \lambda - x^E$. Here, we can observe either a saddle-node bifurcation when $E = 2$ (or, more generally, for any even E corresponding to the merging of multiple states), or an inflection point when E is odd. We have that $f'(x) = -Ex^{E-1}$, and if we evaluate the derivative at the equilibrium point $\lambda^{1/E}$, we have that $f'(\lambda^{1/E}) = -E\lambda^{(E-1)/E}$. Our variance at the equilibrium point is then given by Scheffer et al. (2009):

$$\gamma^2 = \mathrm{Var}(\Delta x) = \frac{\sigma^2}{2E}\frac{1}{(\lambda - \lambda_c)^{\frac{E-1}{E}}} \propto \frac{1}{(\lambda - \lambda_c)^{\frac{E-1}{E}}}, \tag{8}$$

and our more general indicator must take into account the exponent E (Equation 9):

$$A|\lambda| = \left(\frac{\sigma^2}{4E\mathrm{Var}(\Delta X)}\right)^{-\frac{E}{E-1}}, \tag{9}$$

where the multiplicative factors can be neglected because they only scale the indicator and therefore does not influence the prediction.

This formula is a generalization of Equation 6, that can be obtained assuming $E = 2$. When remote from the bifurcation point, higher order exponents dominate, so the variance depends on the degree E of the equation and therefore the formula assuming $E = 2$ may be an unreliable predictor for the critical threshold.

Assuming smooth polynomial transitions, setting $E = 2$ implicitly rules out the existence of other stable states and therefore results in a runaway climate trajectory once tipping occurs. However, using a quadratic polynomial can still produce additional stable states if a discontinuity in its derivative is introduced (see, for example, Rahmstorf et al., 2005). In contrast, modeling the underlying branch with a cubic polynomial with inflection [$E = 3$, also sometimes considered as tipping phenomenon, see Armstrong McKay et al. (2022)] provides a more realistic representation. This choice resolves the limitations of the quadratic form and is consistent with established models such as those in Stommel (1961) and Cessi (1994), which also employ a third-degree formulation. Additionally, the choice of a cubic model can represent the tipping or non-tipping phenomenon as an emergent phenomenon. Equation 8 shows also that critical slowing down and asymptotically increasing variance can be present also if the system only has an inflection point associated with rapid but reversible transition such as, for example, when $E = 3$. Due to the linearization used to derive the variance and autocorrelation characteristics at the tipping point (Scheffer et al., 2009), variance estimation may fail near λ_c for several reasons. These include autocorrelation timescales extending beyond the available data window or the curvature of the equilibrium state with respect to the control parameter, which would cause fluctuations to be more skewed and therefore responding asymmetrically (Guttal and Jayaprakash, 2008; Xie et al., 2019). As a result, the variance calculation may be altered by this asymmetry. In any case, for a reliable prediction, the variance should ideally become arbitrarily large to compute his asymptote, but this is an effect of the approximation. Far away from the tipping point, we cannot make assumptions about the underlying model, since the behavior of the system may deviate significantly from that of a canonical saddle-node bifurcation. In such regions, other dynamical mechanisms or higher-order nonlinearities may dominate, leading to dynamics that are not well captured by simplified bifurcation-based models.

Methods that rely on statistical indicators, such as variance or the AC(1) extrapolation discussed in Section 2.4, require the use of windowed indicators when applied to time series. When evaluating statistical indicators, the theoretical results are hard to apply because we generally have only a single realization of a climatic phenomenon, while indicators such as variance would require multiple realizations of the same phenomenon to be computed. A common approach to solve this issue is to use a sliding variance window of fixed size. The variance window is moved across the domain of available points (Scheffer et al., 2009). The result of this operation is a time series of variance estimates. As implemented in Ditlevsen and Ditlevsen (2023), we align the estimate in a window with the central point. For instance, the variance condenses the information within a moving window into a single value, which inevitably entails some loss of temporal detail. Consequently, any estimate of the variance must account for the window length as a source of sampling uncertainty. Short windows provide too few data points for reliable estimation, leading to high sampling variability. Conversely, long windows may smooth over or fail to detect gradual changes in variance over time. Despite these limitations, we adopt the methodology from Ditlevsen and Ditlevsen (2023) as a test case for this analysis, while acknowledging the potential trade-offs associated with window length.

2.7 Statistical models

We describe the effect of model choice on the maximum likelihood estimation, a statistical approach used to estimate parameters of a probability distribution that best explain observed data. In the context of predicting critical thresholds, such as those associated with the AMOC, maximum likelihood estimation (MLE) can be applied to fit probabilistic models such as polynomial approximations to empirical observations of system behavior. In particular, fitting a polynomial to SPG SST data can highlight the location of critical points in the system, thereby offering insights into potential tipping dynamics. In the literature, MLE of SPG SST data has been applied assuming a quadratic threshold model ($E = 2$, Deg2). This approach implicitly assumes the existence of a critical tipping point, such that the system exhibits a runaway trajectory once the threshold is crossed. However, such a specification also rules out the possibility of additional stable states unless discontinuities are introduced in the derivative.

To test the robustness of this assumption, we extend the analysis to include alternative model formulations. Specifically, we consider:

- Linear model **(Deg1):**

$$dX_t = -(A(X_t - m) + \lambda_t)\, dt + \sigma\, dB_t \tag{10}$$

  Assumes linear drift toward the stable state.
- Quadratic model / saddle-node normal form **(Deg2):**

$$dX_t = -(A(X_t - m)^2 + \lambda)\, dt + \sigma\, dB_t \tag{11}$$

  Assumes a bifurcation near a critical threshold; the stable state (also signature of equilibrium) is given by

$$m = \mu - (|\lambda|/A)^{1/2}. \tag{12}$$

- Cubic model **(Deg3):**

$$dX_t = -(A(X_t - m)^3 + C(X_t - m) + \lambda_t)\, dt + \sigma\, dB_t \tag{13}$$

  A general cubic drift allowing more complex equilibrium structures, including multiple turning points. In particular, if C is negative, we obtain a proper bifurcation; if $C = 0$, we have an inflection point (as in model Deg3B); and if C is positive, the model exhibits a smooth transition without critical points.
- Cubic-inflection model **(Deg3B):**

$$dX_t = -(A(X_t - m)^3 + \lambda_t)\, dt + \sigma\, dB_t \tag{14}$$

  Captures reversible, inflection-like transitions; the stable state is Equation 15

$$m = \mu - (|\lambda|/A)^{1/3}. \tag{15}$$

In the models at Equations 10, 11, 13, 14, λ is the unique control parameter of the system, μ is the stable fixed point of the drift, A and C are model parameters. In particular, A represents a timescale parameter, B_t a realization of Brownian motion, σ^2 scales the variance and m represents the stable state m close to the critical threshold. Deg2 is the model used Ditlevsen and Ditlevsen (2023), assuming a saddle-node bifurcation and predicting a critical threshold in 2065. The mathematical calculations used to obtain the flows for the models are included in the Supplementary Section 2.

The forcing is considered stationary before 1924 and linear thereafter, since Ditlevsen and Ditlevsen (2023) shows that stationarity prevails prior to 1924, allowing the system to be approximated by a stable state with fluctuations around it (ramping). Therefore, in our analysis, we neglect this effect by removing all data values before 1924.

By fitting multiple models with MLE, we aim to evaluate whether the data are informative enough to distinguish between these hypotheses. If all models produce comparable fits, this would indicate that the dataset alone does not provide sufficient resolution to determine the presence or absence of bifurcations, even if the models themselves are physically motivated. This approach allows us to explicitly test the assumptions underlying previous analyses and explore the limits of inference given the quality of available observations.

3 Results

3.1 Polynomials are not suitable models for the AMOC

Ideally, observational data can be represented using simple polynomial models; however, this is not always feasible. To illustrate this limitation, we design a simple experiment, which serves also as a soft criterion to differentiate models that can give a good fit from the data. Our aim is to determine whether simple polynomial models can adequately capture the long-term dynamics associated with the low-frequency components of the AMOC and whether they are capable of representing nonlinearities associated with potential tipping behavior. We analyze the SPG SST dataset and other model output, we detrend it using low-pass filtering techniques before polynomial fitting. The underlying assumption is that if the signal consists only of noise and externally forced variability, with the forcing resembling a polynomial trend, then a purely polynomial component should be readily separable using filtering methods. However, we show that the intrinsic structure of the signal cannot be easily reduced to a polynomial. Certain charateristics of the AMOC which are reflected in the data, such as interannual variability occurring at intermediate timescales, remain present in the signal. This residual variability can bias statistical indicators and reduce the accuracy of polynomial approximations, increasing uncertainty in analyses based on polynomial assumptions. This variability renders statistical analyses based on polynomial assumptions more uncertain, since any polynomial fit would inherently capture part of the non-polynomial change.

We perform polynomial fits on the detrended data. In these approximations, the AMOC index is used as the input variable, while the forcing variable serves as the output. For frequencies up to $1/y$, we detrend the SPG SST data by removing higher-frequency components and subsequently compute polynomial fits of degrees up to three. The experiment assumes that the system remains along a stable branch, with deviations occurring only at frequencies below the cutoff. Figure 1 shows, for each polynomial degree, the fit that yields the lowest residual error.

Figure 1 shows that the cubic polynomial, unlike the quadratic one, provides no indication of an impending transition, suggesting that the SPG SST data (first row, Figure 1I) exhibit no tipping behavior. The failure of both quadratic and cubic polynomials to approximate the underlying branch indicates that variability at intermediate timescales(between the characteristic timescale of branch changes and the timescale of noise) is critical. As a result, polynomial models, whether data driven or theoretically motivated, cannot realistically model the dynamics. The inability of polynomials to capture these intermediate timescales suggests that AMOC dynamics involve more complex interactions than can be represented by simple monotonic trends, and that potential tipping behavior is embedded in variability not well described by polynomials. For the CESM data (second row), the cubic polynomial (Figure 1J) approximates the data relatively well, predicts the tipping point correctly, but fails to capture the structure of the branch accurately (the stable state should jump upward along the stable branch, rather than downward). The quadratic approximation gives a bad fit of the data not predicting correctly the critical threshold. The Cessi model (third column) shows that polynomial approximations provide a worse fit compared to the SPG SST data, suggesting that, because the AMOC behavior is driven more by noise and stochastic diffusion than by critical slowing down, the deterministic component is difficult to separate in the model. Finally, the Cessi model with a faster deterministic component (fourth column) shows that both the quadratic and cubic polynomials (Figures 1H, J, respectively) approximate the data well and correctly predict the theoretical threshold. The cubic approximation also correctly reconstructs the shape of the branch (which entails tipping toward the higher part of the figure).

This result is consistent with the models discussed in Section 2.7, showing that higher- and lower-frequency components cannot be easily separated for the SPG SST data. We note that the filter cutoff frequencies influence the polynomial fits, so the results depend on these methodological choices. Overall, these findings demonstrate that polynomial models are not suitable for representing AMOC dynamics for the SPG SST dataset, as they cannot isolate intermediate-timescale variability, which adds uncertainty in determining tipping behavior. Using polynomial models however, is possible for model data under specific conditions; in particular, in idealized models where the stable state is close to the branch (CESM and Cessi data with faster deterministic component), this methodology can separate the slowly changing state and even reliably predict the critical threshold. We therefore suggest that, for data where a polynomial model could accurately predict a critical threshold, there should exist a cutoff threshold such that the low-frequency components can be approximated by a polynomial.

These findings are directly relevant for EWS-based approaches. If polynomial models fail to isolate the slowly varying branch from intermediate-timescale variability, then extrapolation methods relying on such separation may inherit this structural bias. We therefore next investigate how AR(1)-based extrapolation behaves under different modeling assumptions.

3.2 Results for AR(1) extrapolation

Since the AR(1) extrapolation relies on a theoretical scaling relation involving an exponent E (Equation 8), the predicted tipping time depends critically on this modeling choice. Before evaluating detrending and filtering strategies, we therefore quantify how sensitive the predicted threshold is to the assumed exponent.

We investigate how assumptions about the model exponent, detrending, and filtering affect predicted AMOC thresholds using SPG SST data and the Cessi model. Removing a linear trend from windowed indicators often fails to fully remove shifts in the mean, biasing variance estimates. Polynomial detrending and frequency-based filtering yield different results depending on their settings, illustrating the sensitivity of tipping point predictions to preprocessing choices. We use theoretical AMOC models to highlight these effects and potential pitfalls (see Section 2.5). Detailed results for different detrending strategies and filtering thresholds are presented in Sections 3.2.3, 3.2.4, and we show

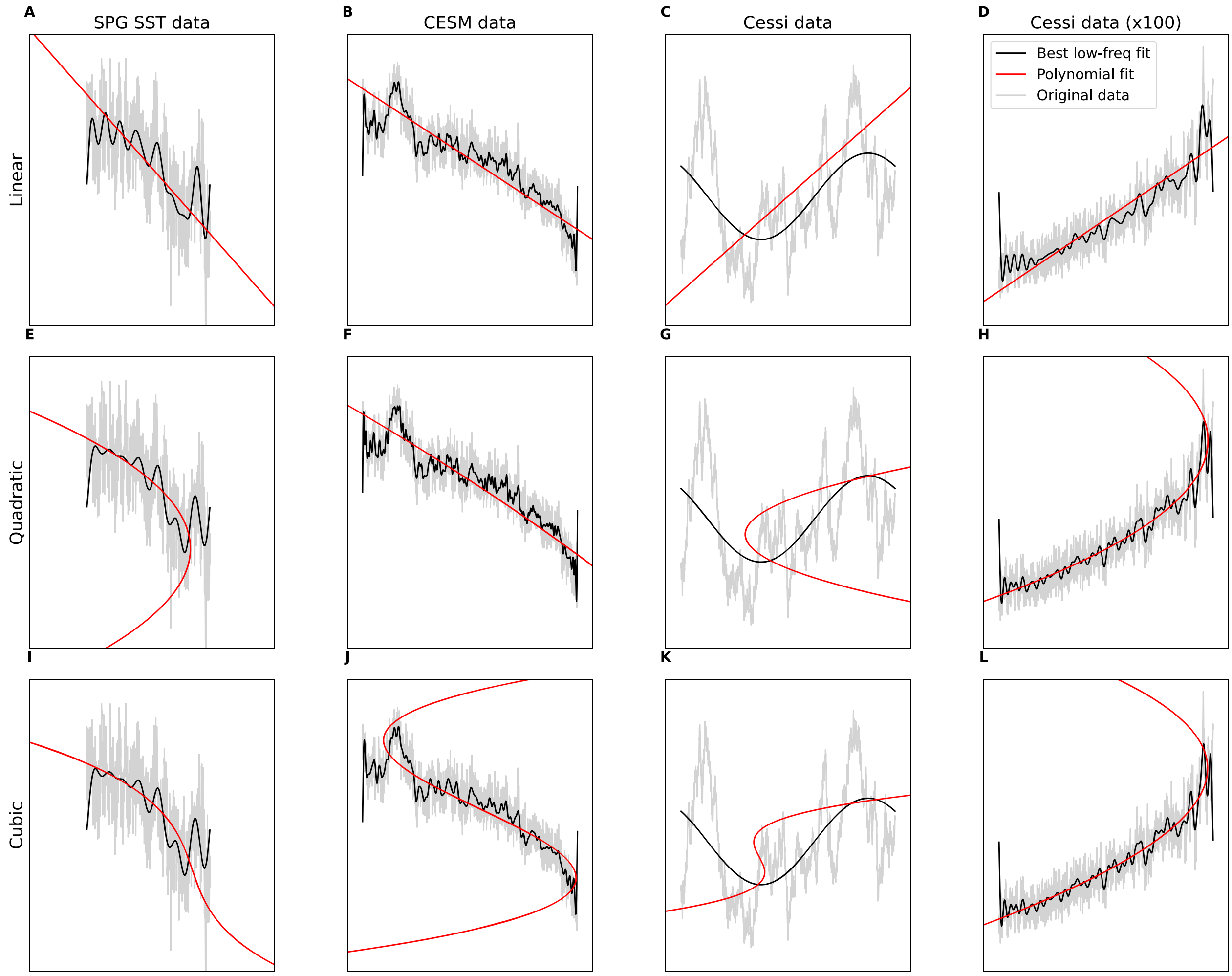

FIGURE 1
Polynomial fits of AMOC strength without higher frequencies. For SPG SST data **(A, E, I)**, CESM data **(B, F, J)**, Cessi data **(C, G, K)** and Cessi data with faster deterministic component **(D, H, L)**, we determine the best-fitting polynomial, measured by the lowest residuals, across varying cut-off thresholds within the interval (0, 1/y]. The polynomial approximations (linear, first row, quadratic, second row and cubic, third row) are computed as functions of the AMOC strength variable, with the output corresponding to the year. The residuals are then calculated for each of the resulting fits.

that polynomial approximations alone poorly approximate filtered signals (see Section 3.1). First, we show that the strong dependence of the predicted threshold on E highlights that preprocessing and detrending choices, which affect the variance estimates in Equation 8, may alter the prediction of the tipping time.

3.2.1 Results for CESM model

Data from CESM, such as the AMOC water transport van Westen et al. (2024), show that specific time intervals can yield realistic estimates of tipping points using AR(1) extrapolation. However, this occurs only in windows where the signal exhibits increasing variance and autocorrelation and low variability. These results are based on a single model realization. As a future extension, we propose repeating this analysis across multiple model runs to assess robustness.

We tested our detrending approach on the these data and found that even a small perturbation (e.g., adding a sine-like increase in AMOC strength lasting 10 years) can produce large discrepancies in the predicted tipping points, as well as differences between second and third degree model fits. Additionally, applying high-pass filtering techniques highlights a sensitivity to the threshold, implying that small changes in the mean state can influence the prediction. Furthermore, these predictions are affected by both the choice of time window and the model. For brevity, the results of these additional experiments are not shown here, as they are already reflected in the analysis of the Cessi models.

3.2.2 Critical threshold prediction assuming different exponent

For the SPG SST data, we estimate the possible thresholds with model exponents between 1.5 and 3.5, starting from the SPG SST data. As shown in Figure 2, the predicted threshold varies substantially with the assumed exponent. Specifically, in the case $E = 2$, corresponding to the normal form of the fold

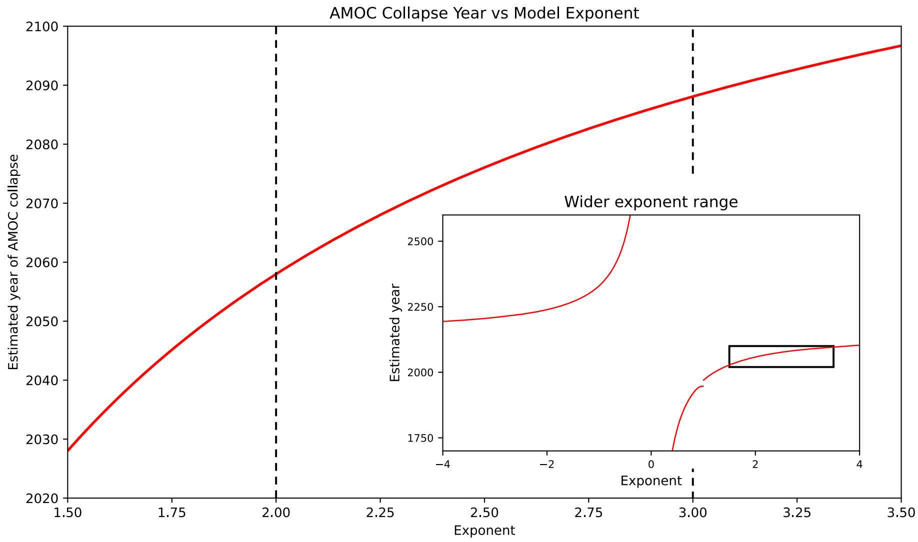

FIGURE 2
Exponent-dependent predicted year of AMOC collapse. For each exponent value $E \in [-4, 4]$, we compute the variance asymptote of the SPG SST data. The larger panel shows a close-up of the interval ($E \in [1.5, 3.5]$). For $E \in \{0, 1\}$, no prediction is available, as the models are inherently linear. In these cases, we obtain an asymptote and a discontinuity, respectively. The degree 2 model corresponds to $E = 2$ and the critical threshold in the year 2057. The exponent $E = 3$ corresponds to the critical threshold (possibly as an inflection) in the year 2088 (the two integer values are highlighted with vertical dashed lines). If E tends to infinity, the estimated critical threshold is the year 2148.

bifurcation, the transition is irreversible and occurs around the year 2057, whereas in the case $E = 3$, it appears around the year 2088 and exhibits a reversible, inflection-like behavior. These differences arise from the sensitivity of the model to the exponent in Equation 8. In this case, we can also obtain that the estimated exponent E is noninteger as the estimated variance might come from the superposition of multiple exponents or from the failure of the formula close to the bifurcation point, so we allow it to be noninteger for the further estimates.

3.2.3 Detrending strategies results

In contrast with the linear detrending typically used in the literature (Lenton et al., 2012; Ditlevsen and Ditlevsen, 2023), we use in our analysis more generic strategies to detrend the data in the form of polynomial detrending, for example by subtracting a third degree polynomial fit to the whole data. Ideally, the detrending should be a polynomial $\lambda = p(x)$ with a degree consistent with a physics-informed model of the system. However, since the SPG SST data result in an ill-conditioned 3rd degree polynomial, we instead consider an estimated polynomial $x = \tilde{p}(\lambda)$. We use this detrending strategy in addition to the assumption-free method of removing a linear trend from the variance window. As already discussed, We found that this approach can lead to earlier estimates for the tipping point, especially if the windows include large fluctuations of the state variable, as in the SPG SST dataset.

The SPG SST data has a state that drifts nonlinearly, and hence, subtracting a linear fit cannot prevent a spurious increase in estimated variance. A linear fit would only be suitable with an equilibrium state changing linearly or very slowly. For example, between 1980 and 2020 the equilibrium state varies considerably and non-monotonically. Using a large window length (e.g., 55 years, as in Ditlevsen and Ditlevsen, 2023) may capture fluctuations caused by interannual variability, leading to larger estimates for the statistical indicators. In principle, eventual critical slowing down should be detectable with larger windows; however, this would only be feasible if the pure noise component (free from the influence of variability) could be separated from the signal. Our suggestion is to detrend the data with higher order polynomial approximations on the whole dataset, or 2nd order or higher polynomial approximations in the considered windows. An assumption on the model degree should ideally be done at this stage to avoid inflating the variance. This assumption implies that the branch corresponding to the correct model degree must be removed from the data in order to separate the noise. However, there are possible issues arising from this mathematically based approach. First, the polynomial approximation may not be defined over some portions of the dataset. This is the case for the AMOC fingerprint, where a quadratic approximation predicts a possible tipping point before the end of the data and is not defined elsewhere (see Figure 1E for reference). Moreover, cubic polynomials may exhibit similar issues, with turning points occurring before the end of the data, such that only the incorrect branch is present for some values of the dataset. We show in Table 1 how different detrending choices affect the critical threshold estimates.

We believe that removing a linear trend is not suitable, since removing degree 2 or 3 in the global trend yield different results from the ones using linear approximation in windows.

Because polynomial detrending still imposes structural assumptions on the signal, we explore whether frequency-based filtering provides a more way to separate slow trends from variability that relies less on assumptions, and how this affects the estimated tipping time.

TABLE 1 Predicted AMOC collapse depending on overall data polynomial detrending degree (DD_{Overall}, horizontal) and window detrending degree (DD_{Window}, vertical).

$DD_{\text{Window}} \backslash DD_{\text{Overall}}$	0	1	2	3
0 (no detrending)	2,031	2,038	2,033	2,049
1	2057	2,057	2,053	2,062
2	2,199	2,199	2,199	2,199
3	2,476	2,476	2,476	2,476

Removing a linear trend from each window corresponds to $DD_{\text{Window}} = 1, DD_{\text{Overall}} = 0$. The estimated threshold corresponds to the AC(1) extrapolation estimates.

3.2.4 Filtering techniques for detrending

To further demonstrate that linear detrending within variance windows is insufficient for removing long term trends from the signal, we apply filtering techniques to the AMOC fingerprint. Our aim is to show that even when more advanced methods are used, the core assumption underlying early warning signal analysis that high frequency variability and noise can be cleanly separated from a slowly varying underlying trend does not hold for the SPG SST data. As discussed in Section 3.2.3, polynomial detrending strategies may remove meaningful slow signals, and thus may not effectively isolate the trends relevant for early warning signals (EWS). To address this, we employ a more advanced approach based on the premise that changes in the system's mean state, including signatures of critical slowing down, are primarily reflected in high-frequency, short-timescale components.

In Figure 3, we illustrate that low-frequency components strongly influence the estimated variance and the predicted timing of approaching the critical threshold, even though, according to theory, only high-frequency fluctuations should contribute to these estimates. Even with linear detrending, these low-frequency components vary considerably within a relatively wide window (e.g., 55 years), consistently increasing statistical indicators and affecting early warning signal estimates.

The variance of the sum of low- and high-frequency components depends not only on their individual variances but also on their covariance. Because these components are correlated, the covariance reflects joint fluctuations, making it difficult to isolate the contribution of low-frequency critical slowing down from other variability. Ignoring this dependence can misrepresent the overall uncertainty in tipping time estimation.

Moreover, the high variability observed in predicted tipping times corresponding to frequencies lower than 0.5/y indicates that accurately estimating the timing of the critical threshold using statistical indicators is highly uncertain. This highlights that filtering strategies must balance removing high-frequency noise while retaining low-frequency signals that carry information about

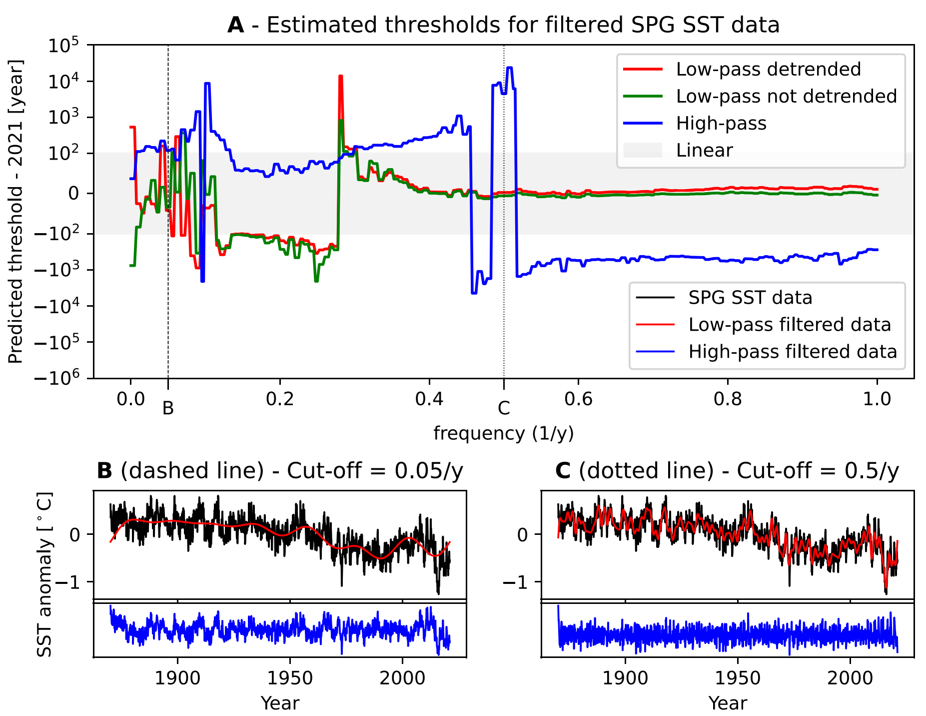

FIGURE 3
AC(1) extrapolation applied to SPG SST data processed with high-pass and low-pass filter with and without linear detrending. Panel **(A)** shows the predicted critical thresholds deviations from 2021 (end of dataset) using low-pass filtering with thresholds up to $1/y$ (red) and the corresponding estimates using the corresponding high-pass filter (blue). We also show the predicted threshold of the low-pass filtering without linear trending (green). A symmetric logarithmic (symlog) scale is used, where values with an absolute magnitude larger than 100 year are displayed on a logarithmic scale, while smaller values ($|y| < 100$) are represented linearly (gray area). Negative values are shown as negative entries on the same scale. Panels **(B)** and **(C)** show the low-pass filtered data with frequencies $0.05/y$ (B, predicted threshold low-pass 1978, 1986 no linear detrending, high-pass 2,141) and $0.5/y$ (C, predicted threshold low-pass 2023, 2015 no detrending, high-pass 6,509). The lower plots in panels B and C show the high-frequency components separated by the SPG SST dataset, they have identical x axis and scaling in the y axis.

10.3389/fclim.2026.1761461

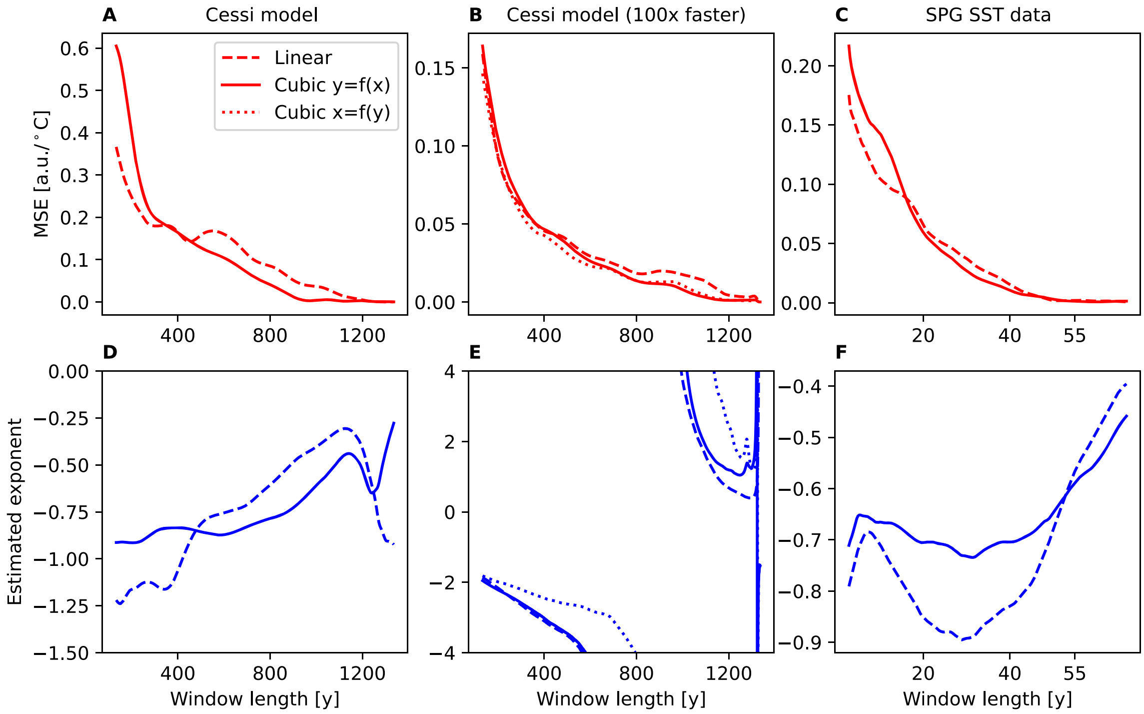

FIGURE 4
Estimated exponent and MSE of fitting depending on variance window. For the Cessi model described in Section 2.5 **(A, D)**, for the version of the model with accelerated deterministic component **(B, E)** and for AMOC SPG SST data **(C, F)**, we estimate MSE **(A–C)** and optimal exponent **(C–E)** of the fits depending on a set of variance windows. We use both the linear detrending in windows described in Ditlevsen and Ditlevsen (2023) and the cubic detrending over the whole domain. In particular, the *x*-axis represents time, while the y axis corresponds to the SPG SST. For all plots, we employ cubic interpolation, considering the SPG SST strength as the dependent variable. For the Cessi model with an accelerated deterministic component, we also apply the interpolation with reversed axes. This procedure is justified because the approximation accurately represents the underlying branch. For the SPG SST data we assume a critical threshold corresponding to the year 2, 057, and we remove the data before 1, 924 so we neglect the ramping time assumed in Ditlevsen and Ditlevsen (2023), where the variance window is 55 years. For the Cessi model, we use the theoretical critical threshold of the model.

critical slowing down. Filters that fail to achieve this separation may lead to biased or imprecise tipping time estimates. We suspect this is the case for the SPG SST data, as polynomial trends cannot be easily separated from the underlying signals.

3.2.5 Estimation of model degree

The previous sections show that both detrending and filtering can largely alter variance estimates and therefore tipping predictions. This raises a deeper question: can the scaling exponent itself be reliably inferred from the data? We therefore estimate the effective model degree directly from variance scaling, using Equation 8.

For both the SPG SST and Cessi data, we assume that we know the critical threshold λ_c. We use the theoretical critical threshold from the Cessi model and assume the year 2057 as reference to represent the critical threshold, based on the results of the AC(1) extrapolation for the SPG SST data.

We estimate the linear fit of $\log(|\lambda - \lambda_c|)$ vs. $\log(\mathrm{Var}(\Delta x))$ and take the estimated coefficient as the optimal exponent E_s. We subsequently compute $E = 1/(1-E_s)$ to fit Equation 8. This process is repeated for all possible variance windows. We show the resulting mean-square error (MSE) of the fit and predicted threshold in Figure 4. In order to minimize the effects of the changing equilibrium state on the variance, we use two different methods to detrend the data. We remove a cubic trend from the whole dataset (cubic in Figure 4) and a linear trend from the window variance (linear in Figure 4, see Ditlevsen and Ditlevsen, 2023). For the Cessi model with accelerated deterministic component, the approximation on the other axis allows a well-conditioned detrending up to almost the critical threshold, we include the corresponding result in Figures 4B, E. An example of these plots can be found in the Supplementary Section 1.

Our estimates of the exponent, illustrated in Figure 4, show that for neither the AMOC SPG SST data nor the Cessi realistic simulated model data we can conclude that with linear detrending the optimal exponent is 2 as it is masked completely by the noise or from the uncertainties in the data for the SPG SST. In the case of the Cessi model, there are some local minima that correspond to estimated exponents smaller than 0, while the cubic detrending predicts approximately the exponent $E = 2$. For the SPG SST dataset, the exponent is never close to 2, nor does the MSE present minima that suggest a good fit for the data for some specific variance window. It appears, however, that in the Cessi model with an accelerated deterministic component, EWS can yield estimated scaling exponents that fall within a realistic range (e.g., 2–3, see Figures 4B, E). Nevertheless, these estimates do not coincide with the window lengths that provide the best statistical fit to the data, nor with those that minimize the mean squared error (MSE). As a result, selecting the EWS window based solely on statistical performance indicators proves to be

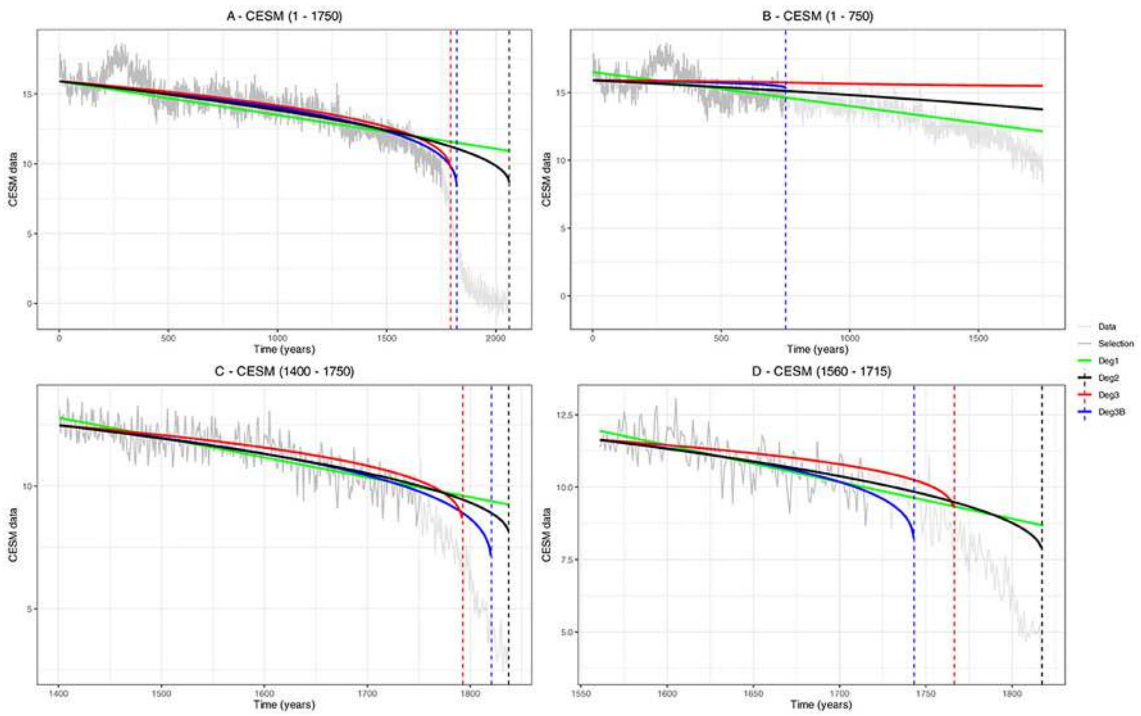

FIGURE 5
Model fits for CESM data, different intervals. Panel **(A)** shows the model fits for CESM data up to the vicinity of tipping (considered as year 1758 of the model simulation). Panel **(B)** shows the fits for the interval restricted up to 750. Similarly, Panels **(C)** and **(D)** show the fits for the model intervals [1, 400, 1, 750] and [1, 560, 1, 715], respectively. The vertical dashed lines indicate the critical thresholds of the respective models.

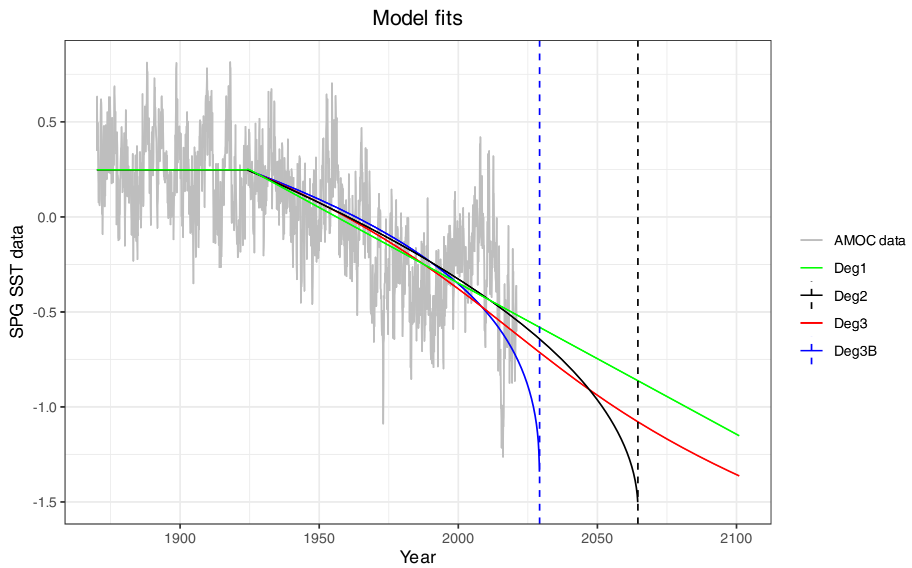

FIGURE 6
Different model fits for SPG SST data. We show that neglecting the data before 1924, the degree 2 model (black), the Deg3 (blue), and the Deg3B model (red) approximate the known data comparably yet predicting completely different future scenarios.

challenging. For the given AMOC data, estimating the theoretical exponent may be challenging due to uncertainties inherent in the data itself and the choice of proxy variables (Ben-Yami et al., 2024). Moreover, a simplified theoretical model may fail to accurately capture the phenomenon since such models often rely on strong assumptions, such as the *a priori* assumption of tipping, which may be limiting when studying a complex system like the AMOC.

3.3 Statistical models

The preceding analyses demonstrate that tipping-time predictions for the SPG SST data depend strongly on structural assumptions: polynomial degree, scaling exponent, detrending method, and filtering threshold. We now compare explicit statistical model formulations to assess how these structural choices translate into different dynamical interpretations.

TABLE 2 Estimated values of model parameters using the Nelder-Mead algorithm with models Deg1, Deg2, Deg3 and Deg3B, with RMSE of the fit.

Version	τ $[y]$	A $[K^{-1}y^{-1}]$	C	m $[K]$	λ_0 $[K^{-1}y^{-3}]$	t_c $[y]$	RMSE
Deg1	0.00	2.44	N/A	0.92	0.00	N/A	0.2387
Deg2	140.56	0.86	N/A	−1.54	−2.73	2064.56	0.2413
Deg3	95.76	0.67	1.61	-0.60	−1.78	N/A	0.2434
Deg3B	105.22	0.34	N/A	−1.48	−1.76	2029.22 (as inflection)	0.2477

3.3.1 Results for CESM data

We test the model fits for results of CESM model (see Section 2.2) To compute the third degree models, we use the technical results described in the Supplementary Section 2. The fits are shown in Figure 5.

From these results on a complex model exhibiting bifurcation behavior, we aim to gain insight into how different models can yield realistic or unrealistic predictions of tipping.

In particular, Figure 5 shows that fitting the whole dataset up to the vicinity of the critical threshold (Figure 5A) leads to good estimates of the critical threshold for the cubic models, whereas the quadratic model exhibits lower fit quality. Figure 5B shows that under conditions of high variability, polynomial fits are generally characterized by low fit quality and can yield unreliable predictions of the critical threshold (we believe this case may be similar to the SPG SST data). Figure 5C shows that if only data from the final part of the branch are considered, realistic predictions can be obtained; however, the cubic models still outperform the quadratic one. Finally, Figure 5D shows that, for intervals comparable to those of the SPG SST data (approximately 150 years of past data with tipping about 50 years in the future, using yearly data in contrast to the monthly SPG SST dataset), the cubic polynomials again perform better than the quadratic one. However, even in this case, the system's variability prevents a precise estimation of the critical threshold.

3.3.2 Results for SPG SST data

Having evaluated the behavior of different model formulations in the controlled CESM setting, where the existence of a bifurcation is known, we now apply the same modeling approaches to the observational SPG SST dataset. This comparison allows us to assess whether similar structural consistency emerges in real data. We include the results of the estimated critical threshold on the SPG SST data using the different versions in Table 2.

We can see clearly that the models predict different behavior of the AMOC. Deg1 shows a linear fit that cannot show bifurcation. In the case of Deg3 and Deg3B, we have respectively no critical point (given by the positivity of C, see Table 2) and an inflection-like transition corresponding to a rapid but reversible change in 2029. Figure 6 suggests that the polynomial models exhibit comparable RMSE values, as summarized in Table 2, making it impossible to select a clearly superior model. While the linear fit provides a slightly better approximation overall, it still fails to capture important variability, such as that occurring after 2000, and therefore does not provide a suitable method for detrending the data, as discussed in Section 3.2.3. This may indicate that while the models perform similarly in terms of minimizing overall error, they can fail to provide an adequate prediction. Consequently, alternative functional forms or modeling approaches may be required to achieve more reliable forecasts that are compatible with the results in Ben-Yami et al. (2024) concerning uncertainty in estimates of critical thresholds. It is likely that the polynomial predictions of the AMOC critical threshold provides a too simplistic description of the complex phenomenon of the AMOC.

4 Discussion

4.1 AMOC modeling approaches and limitations

In studying the stability of the AMOC, different modeling approaches have been proposed. These approaches range from conceptual models with few degrees of freedom to high-resolution coupled climate models. While models with lower complexity predict tipping behavior of the AMOC (Stommel, 1961; Cessi, 1994; Rahmstorf et al., 2005), models with higher complexity, such as fully coupled models, show more heterogeneous results. Many models exhibit approximately linear behavior where a decline of the AMOC is followed by a recovery in strength (Bryan et al., 2006; Meehl et al., 2013; Jackson et al., 2023), but also permanent changes involving a tipping point have been found (Westen et al., 2024). However, complex models also show that spatial phenomena, such as mesoscale eddies (Hirschi et al., 2020) and local circulation patterns (Colombo et al., 2020), are crucial in AMOC evolution and cannot be seen in low-dimensional models. As a consequence, the effects of these phenomena are necessarily neglected in the one-dimensional data, which compresses all spatial effects in a single variable. There is a trade-off between practicability and realism in AMOC modeling. Although simple models enable EWS analysis, reducing spatial dynamics to a single variable may limit tipping-point detection accuracy relative to high-fidelity simulations.

4.2 Limitations of the saddle-node normal form far from the bifurcation point

To illustrate the limitations of the saddle-node normal form far from a bifurcation point, Figure 7 shows that if we are not near the bifurcation point, cubic polynomials of the form $a_1x^3 + a_2x^2 + a_3x + a_4$ outperform quadratic ones of the form $b_1x^2 + b_2x + b_3$, in the approximation of the branch. Moreover,

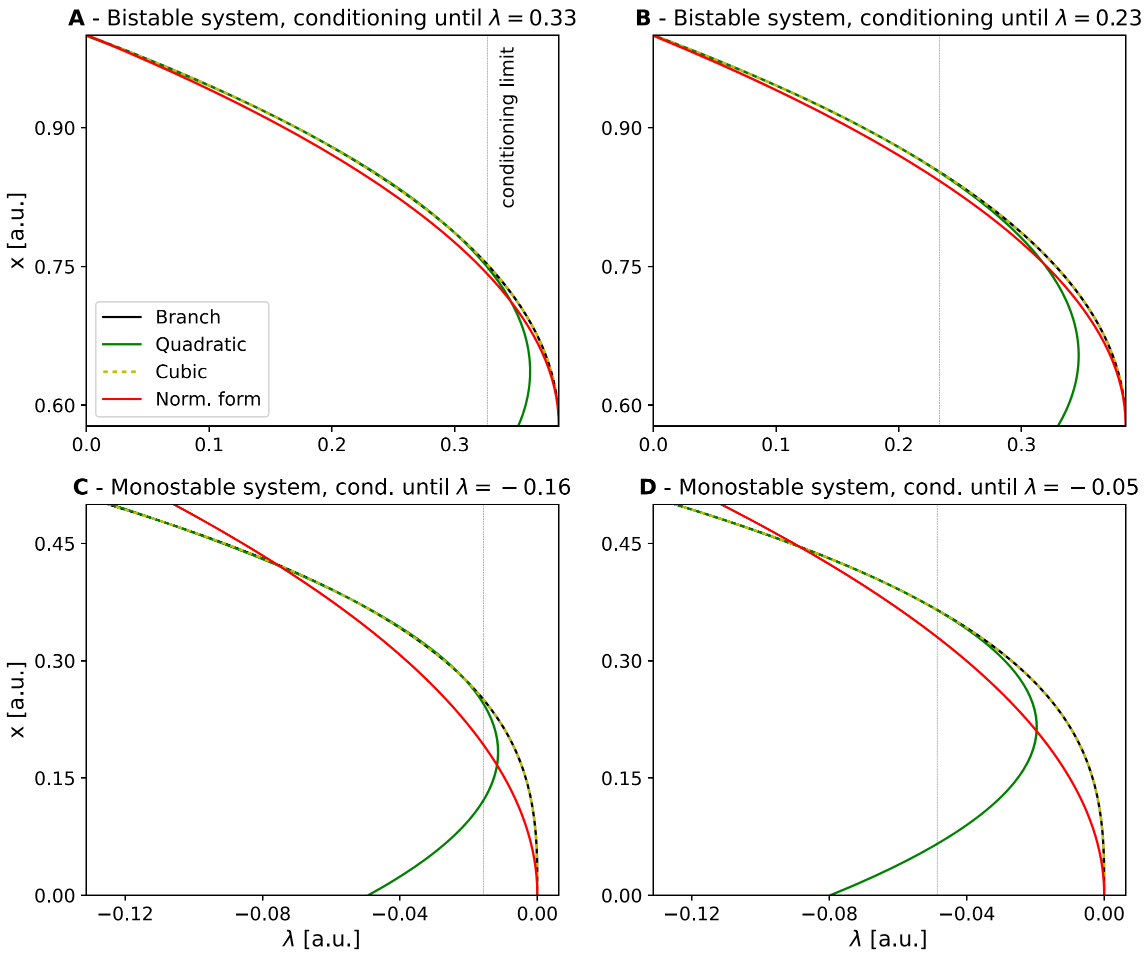

FIGURE 7
Examples of polynomial fits to bistable and monostable systems. Panels **(A)** and **(B)** show a bistable system of the form $x^3 + x + \lambda$ with the critical point corresponding to the bottom right corner in the figure. Panels **(C)** and **(D)** show a monostable system of the form $x^3 + \lambda$ with inflection point in (0, 0). For all figures we show the branch, the best quadratic and cubic approximation and approximating normal form (of a saddle-node bifurcation) that is conditioned to pass through the critical point. We limit the interval conditioning interval of the polynomial fit to part of the available data (up to the vertical line). In the plots, *branch* refers to the polynomial to approximation, *Quadratic* and *Cubic* refer to the polynomial fits used, *Normal form* refers to the normal form with preconditioned critical threshold/inflection point fitted to the data. The Cubic fit overlaps with the branch.

restricting the approximating polynomial to the normal form introduces loss of generality and a priori assumes the presence of a critical threshold.

In Figures 7A, B we have the bistable dynamical system corresponding to the model with deterministic part $x^3 + x + \lambda$ with critical point $\lambda = 2/\sqrt{27}$ corresponding to $x = 1/\sqrt{3}$. This function can represent the branch of stable points of a climatic phenomenon. We also show the polynomial $x^3 + \lambda$ with inflection point $\lambda = x = 0$ (Figures 7C, D). The figure shows that the normal form of the saddle-node bifurcation, conditioned to pass through the critical point, closely approximates the function with a critical threshold, but is not a good approximation for the data featuring an inflection point (Figures 7C, D). However, this result cannot be inferred simply by analyzing the available data. In both cases, it is necessary to condition the fit to ensure that the parabola passes through the known critical point. Additionally, we fit the polynomials to the data up to the critical (or inflection) point using both 2nd and 3rd degree polynomials. Figures 7A–D indicate that, as expected, a general 3rd degree polynomial provides a better fit compared to a general 2nd degree polynomial. Furthermore, cubic polynomials are also effective in distinguishing between the presence (Figures 7A, B) or absence (Figures 7C, D) of a saddle-node bifurcation. We see from Figure 7 that fitting a cubic branch with quadratic polynomials becomes less accurate when fewer interpolation points are used. For this reason, a 2nd degree polynomial can reasonably approximate the model data (e.g., Ditlevsen and Ditlevsen, 2023; Rahmstorf et al., 2005), because the simulations already exhibit complete hysteresis cycles. However, 3rd degree models may be necessary when the system exhibits more complex bifurcation structures, such as multiple turning points or asymmetric hysteresis loops, which cannot be modeled by a simple quadratic approximation.

In the absence of prior knowledge of the critical point, we evaluate the polynomial approximations by simulating scenarios in which the data terminates before reaching the actual bifurcation.

This is in accordance with the finding of Ditlevsen and Ditlevsen (2023), where the critical threshold is predicted to occur around the year 2064, leaving a data gap of approximately 43 years–highlighting the limited temporal coverage available to assess whether the system is already approaching this threshold. This gap highlights a fundamental limitation: given the uncertainty in the available data (Ben-Yami et al., 2024), any attempt to predict the critical threshold requires extrapolation beyond the observed record. Because the record is relatively short, estimates of long-term behavior may be dominated by noise or high-frequency variability rather than the underlying trend. Observing longer-term trends could help mitigate this issue. We propose a sanity check to assess whether the data are suitable for approximation with a given model; this check focuses on how well the dataset can be represented by polynomial models, rather than on the absolute length of the record. Quadratic polynomials systematically misestimate the tipping point compared to the cubic ones, especially when the polynomial fit cannot rely on the data up to the critical threshold as shown in Figures 7B, D, and especially if the critical threshold corresponds to an inflection-like transition. Quadratic polynomials provide a good fit to the available data, but will in any case predict a critical transition for data, also if the transition is not abrupt like in the case of inflection. By contrast, the cubic polynomial in Figure 7 accurately predicts the branch and the critical threshold. Thus, Figure 7 demonstrates that quadratic models, such as those used in the saddle-node bifurcation, may even fail to correctly approximate the branch when higher-order dynamics are present (Strogatz, 2018; Ditlevsen and Ditlevsen, 2023; Ben-Yami et al., 2024). Using Equation 11 as the model and subsequently Equation 12 as the signature of the critical threshold implicitly assumes that a threshold exists.

4.3 Sensitivity in model choice

Across all sections of this manuscript, a consistent theme emerges: the predicted AMOC tipping threshold is highly sensitive to structural modeling assumptions. Whether one varies polynomial degree, scaling exponent, detrending method, filtering threshold, or statistical formulation, the resulting critical time can shift substantially. Choosing the normal form of the saddle-node bifurcation as the baseline model for the data (see Section 4.2) already imposes strong structural assumptions. Selecting the right model for the phenomenon may therefore not be possible from the data alone, or may even be infeasible for a given dataset given the uncertainty in it (Ben-Yami et al., 2024). The second degree model used in Ditlevsen and Ditlevsen (2023) assumes a tipping scenario that may not be present in more general model formulations, nor in reality, and may therefore lead to spurious predictions of an impending critical transition. Similarly, any of the polynomial models considered should not be regarded as uniquely privileged to describe the AMOC future.

We therefore believe that the influence of underlying model assumptions must be explicitly considered when analyzing a signal and searching for tipping behavior. Otherwise, the estimated critical threshold may not be robust, as it can be highly sensitive to the chosen modeling framework. In fact, the actual threshold could differ significantly between alternative models, or it may not exist at all given the available dataset. This highlights the importance of carefully testing how model choice shapes both parameter estimates and the interpretation of system dynamics. We also remark that early warning signals of nonlinear changes in the AMOC are present in the data; however, this manuscript underscores the substantial model uncertainty that accompanies their detection and interpretation. Continuous monitoring and methodological refinement are therefore essential, as they provide not only improved statistical confidence but also a deeper understanding of the mechanisms governing this complex and critical component of the Earth system.

From the extensive analysis of the SPG SST data, we conclude that either the signal-to-noise ratio is insufficient or the intrinsic variability is too high. We see this from our results about statistical indicators, where no model assumption or detrending strategy can be consistently used and also from statistical models, where different degrees and models yield all similar fit quality. In light of this, any single model or technique is likely to underfit an uncertain data series.

4.4 Data limitations and implications for EWS

The results indicate that SPG SST data are highly prone to misinterpretation when used to predict a critical threshold. This issue is also evident in conceptual models, such as the Cessi model, where stochastic generates fluctuations that neither exhibit critical slowing down nor track the system's mean state. A similar pattern is observed in CESM data, where, although the model output generally tracks the main branch of the system, statistical indicators of critical slowing down do not appear uniformly through the signal (van Westen et al., 2024). These uncertainties are reflected in the results of both methods investigated here. In Section 3, we show that AR(1) extrapolation requires the use of an extremely narrow fitting window to produce realistic results, even under optimal conditions. Moreover, even small perturbations in the dataset can lead to unreliable estimates of the threshold (or critical exponent). Likewise, when more complex model-fitting approaches are applied, data variability can cause different models to infer substantially different physical characteristics regarding the future evolution of the phenomenon.

To provide a constructive perspective for future studies, we note that, while datasets should ideally be long enough to capture sufficient variability of the phenomenon under study (however, determining the appropriate data length is not the focus of the present work), a key requirement is that the data should fit a model well. A criterion we propose, as shown in Section 3.1, involves verifying that, for a given time series, it is possible to separate high-frequency components representing noise from low-frequency components representing the underlying model. The SPG SST data do not satisfy this condition; hence, we conclude that predicting a critical threshold from them is not feasible. This conclusion is further supported by the observation that cubic models, which are capable of representing bifurcations for the SPG SST data, show no tipping behavior, while linear models provide comparable fit quality.

5 Conclusions

While it is often very useful to approximate observational data with simple models, the uncertainties in the data are substantial and may result in biased estimates of critical thresholds. Selecting a unique, physically based model from the data alone is not feasible, and even if such a model were identified, its estimates would remain highly uncertain. Assuming a saddle-node bifurcation regardless of the data quality and ignoring other model possibilities will inevitably show the presence of a tipping point. Model choice and detrending possibilities can lead to other biases, each leading to different possible scenarios.

Many other factors contribute to uncertainty, including the choice of onset-of-change factors, the assumption of constant noise forcing, the co-dimension of the bifurcation, the influences external to the model itself, such as uncertainties in climate records, the selection of climatic proxies, future carbon dioxide temperature forcing scenarios (Ben-Yami et al., 2024), or tipping mechanisms (Ashwin et al., 2012; Lohmann and Ditlevsen, 2021; Feudel, 2023; Wang et al., 2023; Chapman et al., 2024). This research, however, raises substantial doubts about the possibility of reliable predictions based on a limited amount of initial uncertainties. While these limitations preclude robust threshold prediction, the presence of non-linear signatures remains informative for monitoring purposes.

Data availability statement

Most of the code used in the analysis presented in this manuscript is adapted from the code in the repositories at https://github.com/TUM-PIK-ESM/tipping_time and in Ditlevsen and Ditlevsen (2023) and is available at Zenodo (10.5281/zenodo.18694383). The datasets analyzed for this study can be found in the Copenhagen university repository https://erda.ku.dk/archives/afce4e1c3ac6f0db61c27cb45c2e9b14/published-archive.html), *AMOC2* data. See Ditlevsen and Ditlevsen (2023) for further information. Additionally, the data for the CESM model can be found at https://zenodo.org/records/10461549 (see van Westen et al., 2024).

Author contributions

AC: Conceptualization, Investigation, Methodology, Software, Visualization, Writing – original draft, Writing – review & editing. EM-N: Methodology, Software, Supervision, Writing – review & editing. MR: Conceptualization, Methodology, Supervision, Writing – review & editing.

Funding

The author(s) declared that financial support was received for this work and/or its publication. This work was supported by the UiT Aurora Centre Program, UiT — The Arctic University of Norway (2025), the Research Council of Norway (project numbers 314570, 350036, and 332901).

Acknowledgments

The authors wish to thank Maya Ben-Yami and Andreas Morr for sharing their repository.

Conflict of interest

The author(s) declared that this work was conducted in the absence of any commercial or financial relationships that could be construed as a potential conflict of interest.

Correction note

This article has been corrected with minor changes. These changes do not impact the scientific content of the article.

Generative AI statement

The author(s) declared that generative AI was used in the creation of this manuscript. Generative AI has been used only to rephrase sentences. Each sentence that has been generated with AI has been carefully checked by the main author.

Any alternative text (alt text) provided alongside figures in this article has been generated by Frontiers with the support of artificial intelligence and reasonable efforts have been made to ensure accuracy, including review by the authors wherever possible. If you identify any issues, please contact us.

Publisher's note

Supplementary material

The Supplementary Material for this article can be found online at: https://www.frontiersin.org/articles/10.3389/fclim.2026.1761461/full#supplementary-material

References

Abrams, J. F., Huntingford, C., Williamson, M. S., Armstrong McKay, D. I., Boulton, C. A., Buxton, J. E., et al. (2023). Committed global warming risks triggering multiple climate tipping points. *Earths Future* 11:e2022EF003250. doi: 10.1029/2022EF003250

Armstrong McKay, D. I., Staal, A., Abrams, J. F., Winkelmann, R., Sakschewski, B., Loriani, S., et al. (2022). Exceeding 1.5°C global warming could trigger multiple climate tipping points. *Science* 377:eabn7950. doi: 10.1126/science.abn7950

Ashwin, P., Wieczorek, S., Vitolo, R., and Cox, P. (2012). Tipping points in open systems: bifurcation, noise-induced and rate-dependent examples in the climate system. *Philos. Trans. A Math. Phys. Eng. Sci.* 370, 1166–1184. doi: 10.1098/rsta.2011.0306

Barry, R. G. (2014). *Essentials of the Earth's Climate System*. Cambridge: Cambridge University Press. doi: 10.1017/CBO9781139583909

Ben-Yami, M., Morr, A., Bathiany, S., and Boers, N. (2024). Uncertainties too large to predict tipping times of major Earth system components from historical data. *Sci. Adv.* 10:eadl4841. doi: 10.1126/sciadv.adl4841

Ben-Yami, M., Skiba, V., Bathiany, S., and Boers, N. (2023). Uncertainties in critical slowing down indicators of observation-based fingerprints of the atlantic overturning circulation. *Nat. Commun.* 14:8344. doi: 10.1038/s41467-023-44046-9

Bloomfield, P. (1976). *Fourier Analysis of Time Series: An Introduction*, revised edition. New York, NY: Wiley.

Boers, N. (2021). Observation-based early-warning signals for a collapse of the Atlantic Meridional Overturning Circulation. *Nat. Clim. Chang.* 11, 680–688. doi: 10.1038/s41558-021-01097-4

Boettiger, C., and Hastings, A. (2012). Early warning signals and the prosecutor's fallacy. *Proc. R. Soc. B Biol. Sci.* 279, 4734–4739. doi: 10.1098/rspb.2012.2085

Bryan, F. O., Danabasoglu, G., Nakashiki, N., Yoshida, Y., Kim, D.-H., Tsutsui, J., et al. (2006). Response of the North Atlantic thermohaline circulation and ventilation to increasing carbon dioxide in CCSM3. *J. Clim.* 19, 2382–2397. doi: 10.1175/JCLI3757.1

Burthe, S. J., Henrys, P. A., Mackay, E. B., Spears, B. M., Campbell, R., Carvalho, L., et al. (2016). Do early warning indicators consistently predict nonlinear change in long-term ecological data? *J. Appl. Ecol.* 53, 666–676. doi: 10.1111/1365-2664.12519

Caesar, L., Rahmstorf, S., Robinson, A., Feulner, G., and Saba, V. (2018). Observed fingerprint of a weakening atlantic ocean overturning circulation. *Nature* 556, 191–196. doi: 10.1038/s41586-018-0006-5

Cessi, P. (1994). A simple box model of stochastically forced thermohaline flow. *J. Phys. Oceanogr.* 24, 1911–1920. doi: 10.1175/1520-0485(1994)024<1911:ASBMOS>2.0.CO;2

Cessi, P., and Young, W. R. (1992). Multiple equilibria in two-dimensional thermohaline circulation. *J. Fluid Mech.* 241, 291–309. doi: 10.1017/S0022112092002040

Chapman, R., Sinet, S., and Ritchie, P. D. L. (2024). Tipping mechanisms in a conceptual model of the Atlantic Meridional Overturning Circulation. *Weather* 79, 316–323. doi: 10.1002/wea.7609

Chisholm, R. A., and Filotas, E. (2009). Critical slowing down as an indicator of transitions in two-species models. *J. Theor. Biol.* 257, 142–149. doi: 10.1016/j.jtbi.2008.11.008

Colombo, P., Barnier, B., Penduff, T., Chanut, J., Deshayes, J., Molines, J.-M., et al. (2020). Representation of the Denmark Strait overflow in a *z*-coordinate eddying configuration of the NEMO (v3.6) ocean model: resolution and parameter impacts. *Geosci. Model Dev.* 13, 3347–3371. doi: 10.5194/gmd-13-3347-2020

Dakos, V., and Bascompte, J. (2014). Critical slowing down as early warning for the onset of collapse in mutualistic communities. *Proc. Nat. Acad. Sci.* 111, 17546–17551. doi: 10.1073/pnas.1406326111

Dakos, V., Carpenter, S. R., Brock, W. A., Ellison, A. M., Guttal, V., Ives, A. R., et al. (2012). Methods for detecting early warnings of critical transitions in time series illustrated using simulated ecological data. *PLoS ONE* 7:e41010. doi: 10.1371/journal.pone.0041010

Dakos, V., Carpenter, S. R., van Nes, E. H., and Scheffer, M. (2015). Resilience indicators: prospects and limitations for early warnings of regime shifts. *Phil. Trans. R. Soc. B Biol. Sci.* 370:20130263. doi: 10.1098/rstb.2013.0263

Ditlevsen, P., and Ditlevsen, S. (2023). Warning of a forthcoming collapse of the Atlantic meridional overturning circulation. *Nat. Commun.* 14:4254. doi: 10.1038/s41467-023-39810-w

Ditlevsen, P. D., and Johnsen, S. J. (2010). Tipping points: early warning and wishful thinking. *Geophys. Res. Lett.* 37:L19703. doi: 10.1029/2010GL044486

Feudel, U. (2023). Rate-induced tipping in ecosystems and climate: the role of unstable states, basin boundaries and transient dynamics. *Nonlin. Process. Geophys.* 30, 481–502. doi: 10.5194/npg-30-481-2023

Guttal, V., and Jayaprakash, C. (2008). Changing skewness: an early warning signal of regime shifts in ecosystems. *Ecol. Lett.* 11, 450–460. doi: 10.1111/j.1461-0248.2008.01160.x

Hirschi, J. J.-M., Barnier, B., Böning, C., Biastoch, A., Blaker, A. T., Coward, A., et al. (2020). The Atlantic Meridional Overturning Circulation in high-resolution models. *J. Geophys. Res. Oceans* 125:e2019JC015522. doi: 10.1029/2019JC015522

Jackson, L. C., de Alastrué, E., Asenjo, K., Bellomo, G., Danabasoglu, H., Haak, A., et al. (2023). Understanding AMOC stability: the North Atlantic hosing model intercomparison project. *Geosci. Model Dev.* 16, 1975–1995. doi: 10.5194/gmd-16-1975-2023

Jackson, L. C., Kahana, R., Graham, T., Ringer, M. A., Woollings, T., Mecking, J. V., et al. (2015). Global and European climate impacts of a slowdown of the AMOC in a high resolution GCM. *Clim. Dyn.* 45, 3299–3316. doi: 10.1007/s00382-015-2540-2

Kéfi, S., Dakos, V., Scheffer, M., Van Nes, E. H., and Rietkerk, M. (2013). Early warning signals also precede non-catastrophic transitions. *Oikos* 122, 641–648. doi: 10.1111/j.1600-0706.2012.20838.x

Kriegler, E., Hall, J. W., Held, H., Dawson, R., and Schellnhuber, H. J. (2009). Imprecise probability assessment of tipping points in the climate system. *Proc. Nat. Acad. Sci.* 106, 5041–5046. doi: 10.1073/pnas.0809117106

Lenton, T. M. (2013). What early warning systems are there for environmental shocks? *Environ. Sci. Policy* 27, S60–S75. doi: 10.1016/j.envsci.2012.06.011

Lenton, T. M., Held, H., Kriegler, E., Hall, J. W., Lucht, W., Rahmstorf, S., et al. (2008). Tipping elements in the earth's climate system. *Proc. Nat. Acad. Sci.* 105, 1786–1793. doi: 10.1073/pnas.0705414105

Lenton, T. M., Livina, V. N., Dakos, V., Van Nes, E. H., and Scheffer, M. (2012). Early warning of climate tipping points from critical slowing down: comparing methods to improve robustness. *Philos. Trans. A Math. Phys. Eng. Sci.* 370, 1185–1204. doi: 10.1098/rsta.2011.0304

Lohmann, J., and Ditlevsen, P. D. (2021). Risk of tipping the overturning circulation due to increasing rates of ice melt. *Proc. Nat. Acad. Sci. USA.* 118:e2017989118. doi: 10.1073/pnas.2017989118

Lux, K., Ashwin, P., Wood, R., and Kuehn, C. (2022). Assessing the impact of parametric uncertainty on tipping points of the atlantic meridional overturning circulation. *Environ. Res. Lett.* 17:075002. doi: 10.1088/1748-9326/ac7602

Meccia, V. L., Simolo, C., Bellomo, K., and Corti, S. (2023). Extreme cold events in Europe under a reduced AMOC. *Environ. Res. Lett.* 19:014054. doi: 10.1088/1748-9326/ad14b0

Meehl, G. A., Washington, W. M., Arblaster, J. M., Hu, A., Teng, H., Kay, J. E., et al. (2013). Climate change projections in CESM1(CAM5) compared to CCSM4. *J. Clim.* 26, 6287–6308. doi: 10.1175/JCLI-D-12-00572.1

Milkoreit, M., Boyd, E., Constantino, S. M., Hausner, V. H., Hessen, D. O., Kääb, A., et al. (2024). Governance for earth system tipping points – a research agenda. *Earth Syst. Gov.* 21:100216. doi: 10.1016/j.esg.2024.100216

Nazarimehr, F., Jafari, S., Perc, M., and Sprott, J. C. (2020). Critical slowing down indicators. *Europhys. Lett.* 132:18001. doi: 10.1209/0295-5075/132/18001

Rahmstorf, S. (2024). Is the atlantic overturning circulation approaching a tipping point? *Oceanography* 37, 16–29. doi: 10.5194/egusphere-egu24-22395

Rahmstorf, S., Crucifix, M., Ganopolski, A., Goosse, H., Kamenkovich, I., Knutti, R., et al. (2005). Thermohaline circulation hysteresis: a model intercomparison. *Geophys. Res. Lett.* 32:L23605. doi: 10.1029/2005GL023655

Rietkerk, M., Skiba, V., Weinans, E., Hébert, R., and Laepple, T. (2025). Ambiguity of early warning signals for climate tipping points. *Nat. Clim. Chang.* 15, 479–488. doi: 10.1038/s41558-025-02328-8

Ritchie, P., and Sieber, J. (2017). Probability of noise- and rate-induced tipping. *Phys. Rev. E* 95:052209. doi: 10.1103/PhysRevE.95.052209

Scheffer, M., Bascompte, J., Brock, W. A., Brovkin, V., Carpenter, S. R., Dakos, V., et al. (2009). Early-warning signals for critical transitions. *Nature* 461, 53–59. doi: 10.1038/nature08227

Stommel, H. (1961). Thermohaline convection with two stable regimes of flow. *Tellus* 13, 224–230. doi: 10.3402/tellusa.v13i2.9491

Strogatz, S. H. (2018). *Nonlinear Dynamics and Chaos: With Applications to Physics, Biology, Chemistry, and Engineering*. Boca Raton, FL: CRC Press. doi: 10.1201/9780429399640

van Westen, R. M., Kliphuis, M., and Dijkstra, H. A. (2024). Physics-based early warning signal shows that amoc is on tipping course. *Sci. Adv.* 10:eadk1189. doi: 10.1126/sciadv.adk1189

Wang, S., Foster, A., Lenz, E. A., Kessler, J. D., Stroeve, J. C., Anderson, L. O., et al. (2023). Mechanisms and impacts of earth system tipping elements. *Rev. Geophys.* 61:e2021RG000757. doi: 10.1029/2021RG000757

Westen, R. M. v., Jacques-Dumas, V., Boot, A. A., Dijkstra, H. A. (2024). The role of sea ice insulation effects on the probability of AMOC transitions. *J. Clim.* 37, 6269–6284. doi: 10.1175/JCLI-D-24-0060.1

Xie, X., He, W., Gu, B., Mei, Y., and Wang, J. (2019). The robustness of the skewness as an early warning signal for abrupt climate change. *Int. J. Climatol.* 39, 5672–5687. doi: 10.1002/joc.6179